lizing enzymes in mice lacking the peroxisome proliferator-activated receptor α (PPARα). J Biol Chem 1998;273:5678–84.
18. Lee SS, Pineau T, Drago J, Lee EJ, Owens JW, Kroetz DL, Fernandez-Salguero PM, Westphal H, Gonzalez FJ. Targeted disruption of the α isoform of the peroxisome proliferator-activated receptor gene in mice results in abolishment of the pleiotropic effects of peroxisome proliferators. Mol Cell Biol 1995;15:3012–22.
19. Peters JM, Aoyama T, Cattley RC, Nobumitsu U, Hashimoto T, Gonzalez FJ. Role of peroxisome proliferator-activated receptor α in altered cell cycle regulation in mouse liver. Carcinogenesis 1998; 19:1989–94.
20. Ni R, Tomita Y, Matsuda K, Ichihara A, Ishimura K, Ogasawara J, Nagata S. Fas-mediated apoptosis in primary cultured mouse hepatocytes. Exp Cell Res 1994;215:332–7.
21. Harada S, Watanabe Y, Takeuchi K, Suzuki T, Katayama T, Takebe Y, Saito I, Miyamura T. Expression of processed core protein of hepatitis C virus in mammalian cells. J Virol 1991;65:3015–21.
22. Novikoff AB, Goldfischer S. Visualization of peroxisomes (microbodies) and mitochondria with diaminobenzidine. J Histochem Cytochem 1969;17:675–80.
23. Gurtu V, Kain SR, Zhang G. Fluorometric and colorimetric detection of caspase activity associated with apoptosis. Anal Biochem 1997; 251:98–102.
24. Folch J, Lees M, Sloane Stanley GH. A simple method for the isolation and purification of total lipids from animal tissues. J Biol Chem 1957;226:497–509.
25. Furutani T, Hino K, Okuda M, Gondo T, Nishina S, Kitase A, Korenaga M, Xiao SY, Weinman SA, Lemon SM, Sakaida I, Okita K. Hepatic iron overload induces hepatocellular carcinoma in transgenic mice expressing the hepatitis C virus polyprotein. Gastroenterology 2006;130:2087–98.
26. Cherkaoui-Malki M, Lone YC, Corral-Debrinski M, Latruffe N. Differential proto-oncogene mRNA induction from rats treated with peroxisome proliferators. Biochem Biophys Res Commun 1990; 173:855–61.
27. Ledwith BJ, Johnson TE, Wagner LK, Pauley CJ, Manam S, Galloway SM, Nichols WW. Growth regulation by peroxisome proliferators: opposing activities in early and late G1. Cancer Res 1996; 56:3257–64.
28. Rininger JA, Goldsworthy TL, Babishi JG. Time course comparison of cell-cycle protein expression following partial hepatectomy and WY14,643-induced hepatic cell proliferation in F344 rats. Carcinogenesis 1997;18:935–41.
29. Peters JM, Cheung C, Gonzalez FJ. Peroxisome proliferator-activated receptor-α and liver cancer: where do we stand? J Mol Med 2005; 83:774–85.
30. Mandard S, Muller M, Kersten S. Peroxisome proliferator-activated receptor α target genes. Cell Mol Life Sci 2004;61:393–416.
31. Tsutsumi T, Suzuki T, Shimoike T, Suzuki R, Moriya K, Shintani Y, Fujie H, Matsuura Y, Koike K, Miyamura T. Interacton of hepatitis C virus core protein with retinoid X receptor α modulates its transcriptional activity. Hepatology 2002;35:937–46.
32. Tanaka N, Hora K, Makishima H, Kamijo Y, Kiyosawa K, Gonzalez FJ, Aoyama T. In vivo stabilization of nuclear retinoid X receptor α in the presence of peroxisome proliferator-activated receptor α. FEBS Lett 2003;543:120–4.
33. Desvergne B, Wahli W. Peroxisome proliferator-activated receptors: nuclear control of metabolism. Endocr Rev 1999;20:649–88.
34. Ito Y, Sasaki Y, Horimoto M, Wada S, Tanaka Y, Kasahara A, Ueki T, Hirano T, Yamamoto H, Fujimoto J, Okamoto E, Hayashi N, et al. Activation of mitogen-activated protein kinases/extracellular signal-regulated kinases in human hepatocellular carcinoma. Hepatology 1998;27:951–8.
35. Masahi T, Shiratori Y, Rengifo W, Igarashi K, Yamagata M, Kurokohchi K, Uchida N, Miyauchi Y, Yoshiji H, Watanabe S, Omata M, Kuriyama S. Cyclins and cyclin-dependent kinases: comparative study of hepatocellular carcinoma versus cirrhosis. Hepatology 2003;37:534–43.
36. Nardone G, Romano M, Calabro A, Pedone PV, de Sio I, Persico M, Budillon G, Bruni CB, Riccio A, Zarrilli R. Activation of fetal promoters of insulin-like growth factors II gene in hepatitis C virus-related chronic hepatitis, cirrhosis, and hepatocellular carcinoma. Hepatology 1996;23:1304–12.
37. Kawate S, Fukusato T, Ohwada S, Watanuki A, Morishita Y. Amplification of *c-myc* in hepatocellular carcinoma: correlation with clinicopathologic features, proliferative activity and p53 overexpression. Oncology 1999;57:157–63.
38. Genini D, Catapano CV. Control of peroxisome proliferator-activated receptor fate by the ubiquitin-proteasome system. J Recept Signal Transduct Res 2006;26:679–92.
39. Moriishi K Okabayashi T, Nakai K, Moriya K, Koike K, Murata S, Chiba T, Tanaka K, Suzuki R, Suzuki T, Miyamura T, Matsuura Y. Proteasome activator PA28γ-dependent nuclear retention and degradation of hepatitis C virus core protein. J Virol 2003;77:10237–49.
40. Li X, Lonard D, Jung SY, Malovannaya A, Feng Q, Qin J, Tsai SY, Tsai M, O'Malley BW. The SRC-3/AIB1 coactivator is degraded in a ubiquitin- and ATP-independent manner by the REGγ proteasome. Cell 2006;124:381–92.
41. Huang H, Starodub O, McIntosh A, Kier AB, Schroeder F. Liver fatty acid-binding protein targets fatty acids to the nucleus. Real time confocal and multiphoton fluorescence imaging in living cells. J Biol Chem 2002;277:29139–51.
42. Dowell P, Peterson VJ, Zabriskie TM, Leid M. Ligand-induced peroxisome proliferator-activated receptor α conformational change. J Biol Chem 1997;272:2013–20.
43. Farinati F, Cardin R, Fiorentino M, D'Errico A, Grigioni W, Cecchetto A, Naccarato R. Imbalance between cytoproliferation and apoptosis in hepatitis C virus related chronic liver disease. J Viral Hepat 2001;8:34–40.
44. Oikawa T, Ojima H, Yamasaki S, Takayama T, Hirohashi S, Sakamoto M. Multistep and multicentric development of hepatocellular carcinoma: histological analysis of 980 resected nodules. J Hepatol 2005;42:225–9.
45. Litwin JA, Beier K, Volkl A, Hofmann WJ, Fahimi HD. Immunocytochemical investigation of catalase and peroxisomal lipid β-oxidation enzymes in human hepatocellular tumors and liver cirrhosis. Virchows Arch 1999;435:486–95.
46. Dharancy S, Malapel M, Perlemuter G, Roskams T, Cheng Y, Dubuquoy L, Podevin P, Conti F, Canva V, Philippe D, Gambiez L, Mathurin P, et al. Impaired expression of the peroxisome proliferator-activated receptor α during hepatitis C virus infection. Gastroenterology 2005;128:334–2.

Research Article **Chromatography**

Received: 31 July 2008, Revised: 7 August 2008, Accepted: 7 August 2008 Published online in Wiley Interscience: 2008

(www.interscience.wiley.com) DOI 10.1002/bmc.1139

Limitation of immunoaffinity column for the removal of abundant proteins from plasma in quantitative plasma proteomics

Tomoko Ichibangase,[a] Kyoji Moriya,[b] Kazuhiko Koike[b] and Kazuhiro Imai[a]*

ABSTRACT: In plasma proteomics, before a proteome analysis, it is essential to prepare protein samples without high-abundance proteins, including albumin, via specific preparation techniques, such as immunoaffinity capture. However, our preliminary experiments suggested that functional changes with use alter the ability of the immunoaffinity column. Thus, in this study, to evaluate the changes of the removal ability of abundant proteins from plasma by the immunoaffinity column, plasma proteome analysis was performed for the long-term test for the reproducibility of the affinity column using the fluorogenic derivatization–liquid chromatography–tandem mass spectrometry method combined with an IgY column. The specific adsorption for albumin decreased with an increase in the number of the column usage before its expiration date. Moreover, it was demonstrated that hydrophobic high molecular weight compounds in plasma adsorbed onto the column materials surface contributed to the functional changes from specific immunoaffinity adsorption into hydrophobic interaction. These results suggested that, in quantitative plasma proteomics studies, it is important to keep in mind the risk of not only the nonselective loss but also the changes in the adsorption ability of the immunoafinity column. Copyright © 2008 John Wiley & Sons, Ltd.

Keywords: plasma; proteomics; immunoaffinity column; abundant protein; FD-LC-MS/MS method

Introduction

Blood samples can be taken at a particular point in time with little burden on patients and the constituents of the blood samples could reflect a developing or existing illness because tissue-specific proteins may be released into the brood stream from the damaged or dead cells. Therefore, it is generally recognized in proteomics studies that blood samples represent the greatest potential source of information on the proteins related to human diseases. However, plasma proteome analysis aiming at quantitative protein profiling and biomarker discovery is not easily done. Since several high-abundance proteins, such as albumin, typically constitute greater than 90% of total protein mass, the detection of lower-abundance proteins which presumably are the biologically interesting population is interfered with by the dominant proteins. To address the complexity of these samples, it is essential to prepare samples via specific preparation techniques to remove high-abundance proteins from the samples before the proteome analysis (Linke *et al.*, 2007; Martosella *et al.*, 2005; Qian *et al.*, 2006; Steel *et al.*, 2003). There are a number of approaches for removing proteins based on their biochemical and biophysical features, such as molecular weight, mass, density, hydrophobicity, surface change and isoelectric point. Among these techniques, immunoaffinity capture using antibodies is rapidly becoming the prefractionation method of choice in proteomics analysis. Commercial kits using an avian immunoglobulin yolk (IgY) have recently become available due to its high avidity and lesser cross-reactivity with heterologous human proteins (Huang *et al.*, 2005; Linke *et al.*, 2007; Qian *et al.*, 2006). A number of researchers have already indicated its utility and the improvement of the detection of low-abundance proteins by the elimination of the high-abundance proteins using the IgY affinity column (Gong *et al.*, 2006; Huang *et al.*, 2005; Linke *et al.*, 2007; Liu *et al.*, 2006; Qian *et al.*, 2006).

We have recently developed a highly sensitive and quantitative proteomics method called fluorogenic derivatization–liquid chromatography–tandem mass spectrometry (FD-LC-MS/MS) (Masuda *et al.*, 2004; Toriumi and Imai, 2003). The method consists of separation of the fluorogenic derivatized proteins by high-performance liquid chromatography (HPLC), isolation of the target protein obtained by HPLC, hydrolysis and identification of the target protein by LC-MS/MS with the probability-based protein identification algorithm. This highly selective, sensitive and reproducible method enables the post-translational proteins and isoforms to be distinguished. The method was applied to the extracts of *Caenorhabditis elegans*, mousee liver and breast cancer cell lines, and revealed the proteins related to early-stage Parkinson's

* Correspondence to: K. Imai, Research Institute of Pharmaceutical Sciences, Musashino University, 1-1-20 Shinmachi, Nishitokyo-shi, Tokyo 202-8585, Japan. E-mail: k-imai@musashino-u.ac.jp

[a] Research Institute of Pharmaceutical Sciences, Musashino University, Tokyo, Japan

[b] Department of Internal Medicine, Graduate school of Medicine, University of Tokyo, Tokyo, Japan

Abbreviations used: DAABD-Cl, 7-Chloro-*N*-[2-(dimethylamino)ethyl]-2,1,3-benzoxadiazole-4-sulfonamide; FD, fluorogenic derivatization; HCCA, α-cyano-4-hydroxycinnamic acid; TCEP, Tris (2-carboxyethyl) phosphine hydrochloride; TFA, trifluoroacetic acid; TOF, time-of-flight.

Contract/grant sponsor: MEXT HAITEKU (2004–2008), Grant-in-Aid for Young Scientists (Start-up).

Contract/grant sponsor: Mochida Memorial Foundation for Medical and Pharmaceutical Research.

disease (Ichibangase *et al.*, 2008), hepatocarcinogenesis (Ichibangase *et al.*, 2007) and tumor progression and metastasis (Imai *et al.*, 2008). During the course of our studies, we applied the FD-LC-MS/MS method to plasma proteomics. To detect plasma biomarkers that are probably masked by the high-abundant proteins, an IgY affinity column was utilized for the removal of the dominant proteins, such as albumin, from plasma before the fluorogenic derivatization (FD) of the plasma proteins. On the preliminary experiments, the quantitative changes of the peaks on the chromatograms obtained from the same samples were observed on every occasion of sample treatment with the affinity column. Since the detectability of the fluorogenic derivatized proteins by the HPLC-fluorescence detector is always constant, the change in the removal ability of the IgY column for the abundant proteins could be monitored during the usage of the column. Although it was reported that there was a risk of loss by inadvertent capture of low-abundance proteins (Bjorhall *et al.*, 2005; Gong *et al.*, 2006; Linke *et al.*, 2007; Plavina *et al.*, 2007; Yocum *et al.*, 2005), there are no reports of long-term tests for the reproducibility of the affinity column in quantitative proteome analysis.

In this study, to evaluate the removal ability of abundant proteins from plasma by the affinity column, we performed proteome analysis of plasma sample and protein standards by FD-LC-MS/MS combined with the IgY technique and investigated the cause of the quantitative changes of the chromatograms mentioned above.

Experimental

Materials and Methods

Reagents. 7-Chloro-*N*-[2-(dimethylamino)ethyl]-2,1,3-benzoxadiazole-4-sulfonamide (DAABD-Cl) and 6.0 M guanidine hydrochloride (pH 8.7 buffer solution) were purchased from Tokyo Chemical Industry (Tokyo, Japan). Ethylenediamine-*N*,*N*,*N*',*N*'-tetraacetic acid sodium salt (Na_2EDTA) and 3-[(3-Cholamidopropyl) dimethyammonio]-1-propanesulfonate (CHAPS) were from Dojindo Laboratories (Kumamoto, Japan). Tris (2-carboxyethyl) phosphine hydrochloride (TCEP) was obtained from Sigma-Aldrich (St Louis, MO, USA). Acetonitrile and trifluoroacetic acid (TFA) for the HPLC-fluorescence detection were HPLC grade and were obtained from Wako Pure Chemical Industries (Osaka, Japan). All other reagents used were of analytical grade.

Affinity Columns

The prepacked IgY-R7 Spin Column and Seppro®-IgY12 were obtained from Beckman Coluter (Fullerton, CA, USA) and GenWay Bioteck (San Diago, CA, USA), respectively. The IgY-R7 Spin Column (1.2 mL spin column) removes seven high-abundance proteins in rodent plasma (albumin, IgG, α2-antitrypsin, IgM, transferring, haptoglobin and fibrinogen) and utilizes centrifugation as the force for affinity separation. The column is said to be reusable 100 times under proper conditions. The Seppro®-IgY12 column is optimized for human plasma and removes 12 high-abundance proteins (IgA, α1-acid glycoprotein, α2-macroglobin, apolipoproteins A-I and apolipoproteins A-II besides the above seven proteins). This column is used with the high-throughput automated proteomic sample processing instrument (Magtration System SA-1; Precision System Science, Chiba, Japan) and is said to be able to be used 30 times. Both companies are corporate partners for the exclusive marketing of the IgY microbeads technology, and both column materials are the same except for recognized animal species to the IgY.

Plasma Samples

For the IgY-R7 Spin Column, plasma sample were obtained from C57BL/6N male mice (10 and 19 months; Clea Japan, Tokyo, Japan) by centrifugation at 5510 rpm for 10 min at 4°C, and frozen at −80°C until use. On the other hand, the human control plasma sample purchased from Sigma-Aldrich was used for the Seppro®-IgY12 column. The control plasma sample was passed through a 0.45 μm filter before use.

Treatment of Mouse Plasma with the IgY-R7 Spin Column

Mouse plasma treated with the spin column was carried out according to the manufacturer-instructed column usage and loading capacity [10 μL plasma diluted with dilution/washing buffer: 10 mM Tris–HCl, 150 mM NaCl, pH 7.4 (TBS)]. Three buffers (dilution/washing buffer; stripping buffer: 100 mM glycine, pH 2.5; neutralization buffer: 100 mM Tris–HCl, pH 8.0) were used under the separation scheme that consisted of sample loading–washing–eluting–neutralization followed by a re-equilibration scheme for a total cycle time of 40 min. To increase the recovery of the non-specific proteins, the resulting flow-though fraction and the washing fractions were collected and concentrated to 10 μL with 3.0 kDa molecular weight cutoff device according to the manufacturer's instructions (Microcon YM-3; Millipore, Billerica, MA, USA).

Treatment of Protein Standards and Control Human Plasma Sample with the Seppro®-IgY12 Column

The molecular weight standards, consisting of phosphorylase B, serum albumin, ovalbumin, carbonic anhydrase, trypsin inhibitor and lysozyme for electrophoresis (Table 1; 12 mg/mL protein amount; low range; Bio-Rad, Herccules, CA, USA), were employed in sample processing without dilution to evaluate the recovery of non-specific proteins from the column. The injected amount of the protein standards was 2.4 mg protein per injection to the affinity column. Since, in the instructions, 15 μL of plasma (generally corresponding to 70–80 mg proteins/mL) was diluted to 500 μL and loaded to the affinity column, the injected amount of the standards was compatible. According to the manufacturer's instructions, the protein standards were set in the sample holding and then the flow-though fraction was obtained.

The control human plasma sample was also treated according to the manual. Briefly, 15 μL of plasma sample was diluted with the dilution/washing buffer to 500 μL, and the sample was set in the sample holding, as in the case of the protein standards. The resulting flow-though fraction of the plasma was concentrated

Table 1. Protein standards and the number of labeled region with DAABD-Cl

Protein	Source	MW (kDa)	No. of rabeled region
Phosphorylase B	Rabbit muscle	97.4	10
Serum albumin	Bovine	66.2	35
Ovalbumin	Hen egg white	45	5
Carbonic anhydrase	Bovine	31	2
Trypsin inhibitor	Soybean	21.5	5
Lysozyme	Hen egg white	14.4	6

to 15 μL with a Microcon YM-3 device. A series cycle including the sample loading–washing–eluting–neutralization finished in 65 min.

FD-LC-MS/MS Conditions

Each FD condition was optimized for the protein standards and for plasma samples in order to obtain the highest peak on the chromatograms. For the protein standards, a 2.5 μL aliquot of the flow-though fraction was mixed with 30 μL of a mixture of 0.83 mM TCEP, 3.3 mM Na_2EDTA and 16.6 mM CHAPS in the pH 8.7 buffer solution, 12.5 μL of the buffer solution and 5.0 μL of 8.0 mM DAABD-Cl in acetonitrile. The mixture was reacted at 50°C for 5.0 min, and the reaction was stopped with 1.5 μL of 20% TFA. A 20 μL aliquot of the above reaction mixture was injected to the HPLC system (Hitachi L-2000 series; Hitachi Instruments, Tokyo, Japan) using a column of Intrada WP-RP (30 nm pore size, 250 × 4.6 mm i.d., Imtakt Co, Kyoto, Japan) at 60°C with a flow rate of 0.55 mL/min. The eluent (A) and eluent (B) were water–acetonitrile–TFA (90:10:0.15, v/v/v) and water–acetonitrile–TFA (30:70:0.05, v/v/v), respectively. The gradient condition was established from 5 to 100% eluent (B) over a period of 60 min. For mouse and control plasma samples, a 6.0 μL aliquot of the flow-though fraction was mixed with 30 μL of the above mixture of TCEP, Na_2EDTA and CHAPS, 10 μL of the buffer solution and 4.0 μL of 825 mM DAABD-Cl in dioxane. After the FD reaction (50°C for 5.0 min), the reaction was stopped with 2.0 μL of 20% TFA. An aliquot (10 μL) of the reaction mixture was injected, and the longer column (Intrada WP-RP 30 nm pore size, 500 × 4.6 mm i.d., Imtakt Co) together with a precolumn (Intrada WP-RP 30 nm pore size, 5.0 × 2.0 mm i.d., Imtakt Co) at 60°C was adopted with a flow rate of 0.55 mL/min on the HPLC system. The mobile phases consisted of water–acetonitrile–TFA (A) 90:10:0.15 and (B) 30:70:0.05. Mobile phase (C) was the same as (A), except with 0.05% TFA. The gradient condition is described in Fig. 1. Fluorescence detection was carried out at 395 and 505 nm for the excitation and emission wavelengths, respectively. The peak height of each protein peak obtained from the HPLC chromatograms was calculated by HITACHI EZChrom Elite™ Chromatography Data System (Hitachi Instruments) and the identification of the standard proteins was accomplished according to the previous report (Ichibangase *et al.*, 2007).

Scanning Electron Microscopy and Matrix-assisted Laser Desorption/Ionization MS Analysis

Scanning electron microscopy (SEM) and matrix-assisted laser desorption/ionization (MALDI) MS analyses were conducted in Jeol Datum (Tokyo, Japan) and Bruker Daltonics Japan (Kanagawa, Japan), respectively.

For SEM analysis, the column materials were diluted with phosphate buffer (300 mOsm) and fixed with fixative (2.5% glutaraldehyde in PBS, pH 7.0) for 10 min. The fixed sample was captured on the filter (SEM-Pore: 0.6 μm i.d.; 10 μm) and washed with the buffer. After the osmium-fix (2% OsO_4) and a brief rinse with the fixative solutions, specimens were dehydrated in a series of graded ethanol (30–100%). The immersed specimens in ethanol were replaced with isoamyl phenylacetate and subjected to critical point drying. The dried samples were coated with osmium using a plasma coater (OPC80N, Jeol). Images were acquired using a Jeol JSM-7401F in normal SEM mode. For the low power microscope images for the whole picture of a material, a lower electron image (LEI) was applied.

For MALDI MS analysis, the column materials were washed and spotted on a plate. α-Cyano-4-hydroxycinnamic acid (HCCA) was used as matrix. MALDI mass spectra were acquired with time-of-flight (TOF) MS (autoflex III, Bruker Daltonics) in positive linear mode.

Results and Discussion

Quantitative Functional Changes of the IgY-R7 Spin Column after a Number of Treatments with Mouse Plasma

For the detection of low-abundance proteins in mouse plasma, the removal of high-abundance proteins from mouse plasma with the affinity column was performed prior to the FD-LC-MS/MS proteome analysis. Typical chromatograms are shown in Fig. 1(A), obtained from the same mouse plasma sample treated with 80 and 86 cycles of the same spin column, respectively. All peak heights obtained from the 86 cycles of the spin column were clearly higher compared with those obtained from the 80 cycles. Although a difference between column lots might exist, there were also significant differences in the removability of the affinity column between the second (column lot no. 2) and the 44th cycles (column lot no. 1) of the treated spin column [Fig. 1(B)]. The relative standard deviation (RSD) of the protein peaks was calculated between-day ($n = 3$) using samples provided by the same treatment number of the column. The RSD values were less than 21.6%, obtained from the peak in Fig. 1(A), suggesting that the detectability of the fluorogenic derivatized proteins by HPLC is constant. Therefore, it was considered that the quantitative changes of the peaks on the chromatograms might result from the changes in the affinity column by the sample treatment.

Evaluation of Seppro®-IgY12 Column for the Adsorption of Protein Standards using an Automatic Instrument

To eliminate a manual usage error from the sample processing, a high-throughput automated instrument, SA-1, for the removal of high-abundance proteins from human plasma samples with a Seppro®-IgY12 column was investigated. For the evaluation of the exact adsorption ratio of specific and non-specific proteins to the affinity column, the affinity column was periodically treated with protein standards after treatment with a control human plasma sample some dozen times. Since the other investigator has reported the non-specific adsorption of the protein by concentration methods such as a centrifugal filter to be about 15% (Linke *et al.*, 2007), the flow-through fraction of the injected protein standards from the affinity column was subjected directly to the FD-LC-MS/MS analysis without a protein concentration step in this study.

At first, to eliminate the non-specific adsorption to the affinity column, the protein standards mixture was divided into two parts and one was subjected into the untreated affinity column, and the flow-though fraction was derivatized with the fluorogenic reagent, DAABD-Cl, and separated by the HPLC system (4.8 μg protein/HPLC injection). Another part of the protein standards mixture was diluted and derivatized with DAABD-Cl, and injected onto the HPLC system (4.8 μg protein/HPLC injection). The obtained chromatograms are depicted in Fig. 2. Each protein peak was collected, digested in peptide mixtures, and identified by applying the peptides to HPLC-MS/MS with a

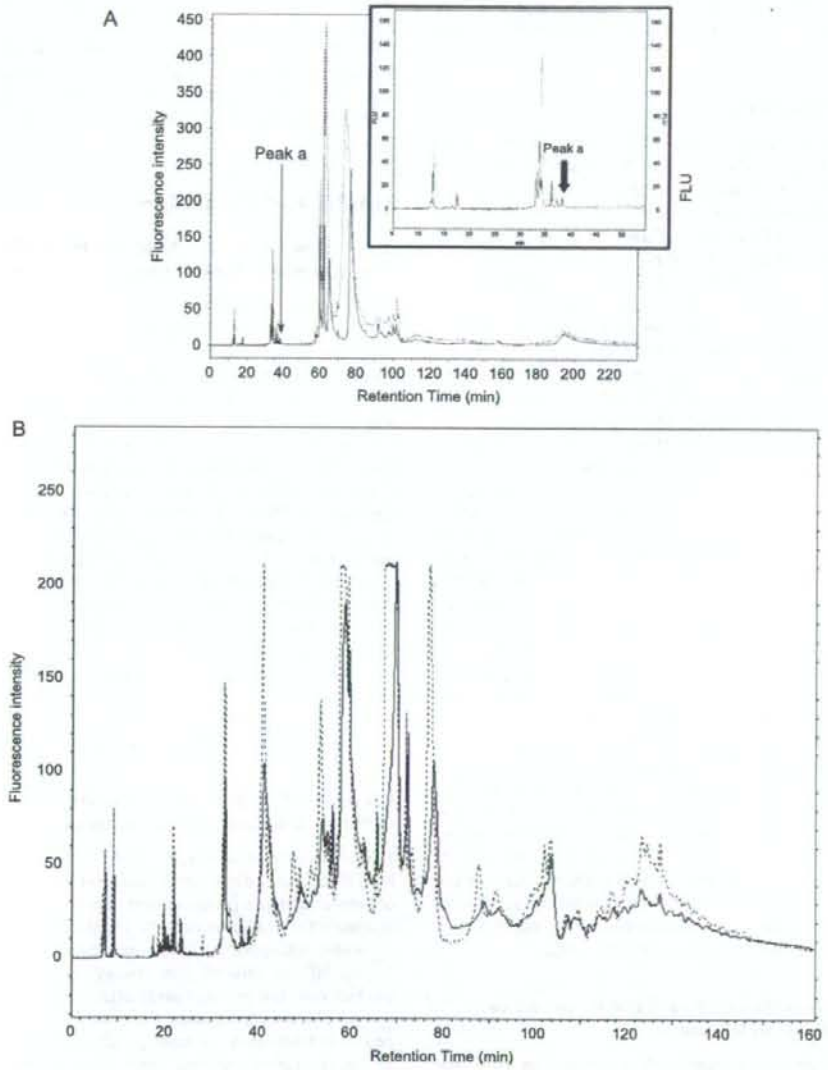

Figure 1. Chromatograms of mouse plasma samples treated with IgY-R7 Spin Columns. (A) The mouse plasma (19 months, C57BL/6N) treated 80 times (solid line) and 86 times (dotted line) in the same spin column. The gradient conditions were as follows: time (min), 0 → 10 → 20 → 44 → 48 → 68 → 80 → 90 → 108 → 120 → 130 → 160 → 180 → 230; B (%): 5 → 5 → 30 → 30 → 35 → 38 → 39.2 → 39.2 → 42 → 43 → 44 → 45 → 47 → 58; C (%): 0 → 0 → 0 → 0 → 0 → 0 → 0 → 60.8 → 58 → 57 → 56 → 55 → 53 → 42. (B) The mouse plasma samples (10 months, C57BL/6N) were treated with the second cycle (column lot no. 2; solid line) and the 44th cycle (column lot no. 1; dotted line) of each spin column. The gradient conditions were as follows: time (min), 0 → 5 → 10 → 22 → 24 → 34 → 54 → 60 → 60.1 → 80 → 130 → 140 → 150 → 160 → 170; B(%): 5 → 5 → 30 → 30 → 35 → 38 → 42 → 43 → 43 → 47 → 58 → 60 → 60 → 75 → 78; C(%): 0 → 0 → 0 → 0 → 0 → 0 → 0 → 0 → 0 → 57 → 53 → 42 → 40 → 40 → 25 → 22.

database-searching algorism. Table 2 shows the adsorption ratio of the proteins to the untreated column and the identified protein names. The protein names of peak 1 and 2 could not be identified since these peaks were peptides coexisting in the protein standards. Also, carbonic anhydrase and ovalbumin could not be detected. Since carbonic anhydrase has only two cycteine residue for labeling with DAABD-Cl, its detection might be difficult. The reason for the undetected ovalbumin was not clear. Since this study was aimed at investigating the changes in the adsorption of the specific and non-specific proteins using the column, this issue was not examined further. Consequently, although the affinity column was able to efficiently remove bovine serum

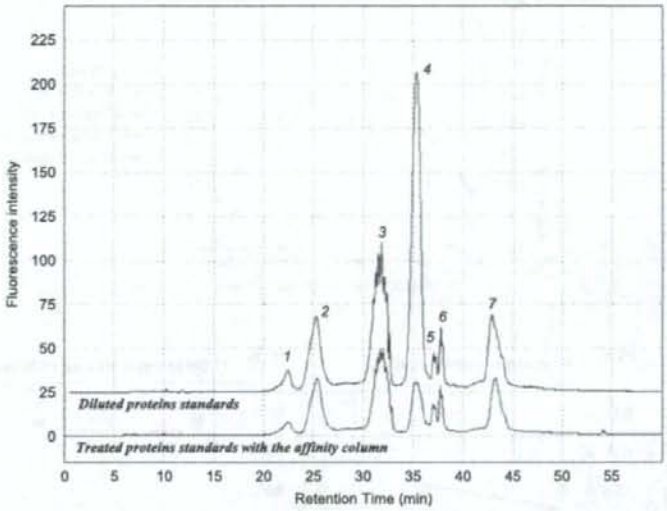

Figure 2. Chromatograms of the protein standards which were treated with Seppro®-IgY12 column and diluted to the same protein amount (4.8 μg/HPLC injection) as the amount for the column treatment. The peak numbers correspond to Table 2.

Table 2. Adsorption ratio to the untreated Seppro®-IgY12 column and protein names obtained by FD-LC-MS/MS method

Peak no.	Adsorption ratio to the untreated Seppro®-IgY12	Protein name
1	38.5%	Peptide
2	30.6%	Peptide
[a]3	45.9%	Lysozyme
4	83.9%	Bovine serum albumin (BSA)
[b]5	18.3%	Trypsin inhibitor
6	28.5%	Trypsin inhibitor
7	30.4%	Phosphorylase B

[a]3, [b]5: Most highest peak

albumin (BSA; 83.9%) as compared with the other proteins in the standards, non-specific binding to the column materials or to carrier proteins such as albumin itself was observed in the 18.3–45.9% range and could result in the loss of presumed biomarkers.

Next, the time series changes of the specific and non-specific adsorption of proteins to the column were investigated. The protein standards mixture was treated with the column periodically after 10 and 20 cycles of treatment of the control plasma sample. The relation of the changes of the protein standards adsorption to the number of uses of the affinity column is shown in Fig. 3(A). The specific adsorption of BSA decreased with an increase in the number of times the column was used. However, the non-specific adsorption for lysozyme, trypsin inhibitor and phosphorylase B reached a maximum at 11 cycles and decreased at 21 cycles. Since the affinity column was optimized for human plasma, the absorption of BSA for the column might be weaker than for plasma albumin. However, the adsorption of albumin in control plasma also decreased with an increase in the number of times the column was used (data not shown). Moreover, since the slopes of decrease differed among the protein standards, the correlation of each adsorption with molecular weight of each protein was calculated [Fig. 3(B)]. The open dots show the value of BSA in Fig. 3(B). The correlation coefficient value was the closest to 1.00 ($R^2 = 0.813$) for 21 cycles [Fig. 3(B-3)], demonstrating that the adsorption ability of the column does not depend any longer on the affinity of the antibody but on the hydrophobicity of the protein. In contrast, the correlation of the values obtained from the first cycle [Fig. 3(B-1); $R^2 = 0.077$] was not fairly observed between the adsorption ability and the hydrophobicity, and the value for BSA was apart from those for other proteins. Therefore, BSA was specifically removed as compared with the other protein standards by the immunoaffinity adsorption. Also, as shown in Fig. 3(B-2), the result obtained from 11 cycles ($R^2 = 0.012$) demonstrated that all proteins bound to the surface of the affinity column materials equally. Therefore, the present data demonstrates that the quantitative changes of the adsorption for the affinity column appear before the limited use of the column (30 times in the manufacturer's instructions).

Understanding the State of the Plasma-treated Column Materials

To understand the state of the column materials of the Seppro®-IgY12 column, the untreated and 11- and 21-times-treated column materials were subjected to electron microscopy and MALDI-TOF-MS analysis.

As shown in Fig. 4, the SEM images show an obvious difference between the untreated and treated materials. The attachment of the unknown bio-molecules to the materials surface appeared and increased with an increase in the number of treatments.

Next, in order to characterize the attached compounds, the same materials were subjected to MALDI-TOF-MS analysis. Since

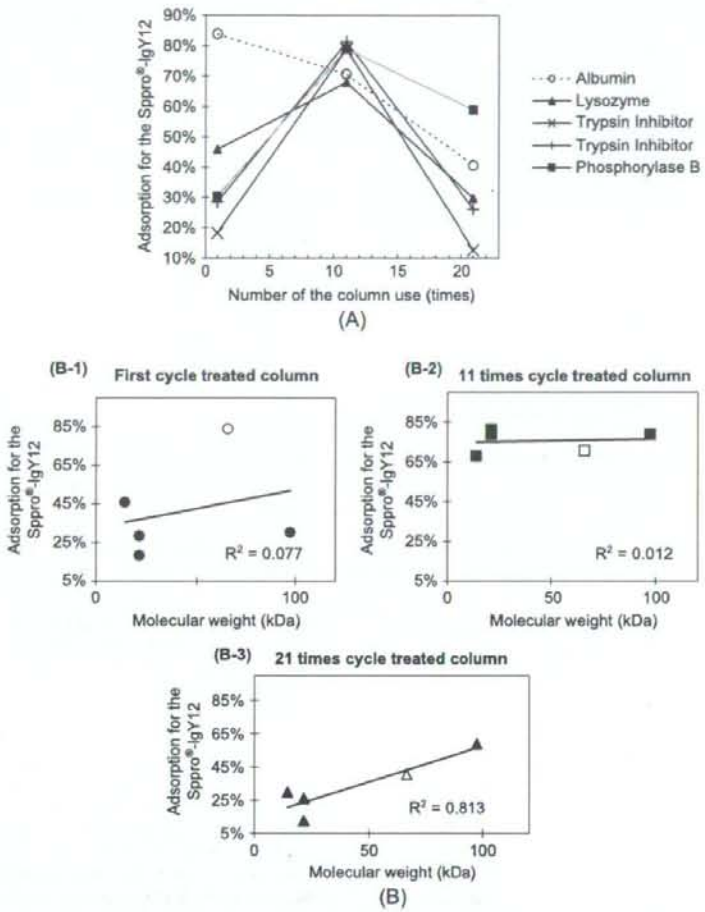

Figure 3. Changes of the adsorption ratio of protein standards for Seppro®-IgY12 column. (A) Relation of the adsorption ratio to the number of times the column was used. (B) Correlation of the adsorption ratio for the column with molecular weight of each protein standard using the column treater one (B-1), 11 (B-2) and 21 (B-3). The open dots show the value for BSA.

direct laser irradiation of the materials could affect the instrument, the positions to be irradiated were the points of the existence of many matrices on a few column materials. Although several peaks existed of less than 70,000 *m/z* in each mass spectrum, the higher molecular weight peaks (7266, 9689, 14,532 and 29,041 *m/z*) appeared in the treated but not in the untreated materials (Fig. 5). After the materials were washed with acetonitrile, the higher molecular weight peaks in the treated materials disappeared (data not shown). Therefore, the compounds attached to the material surface should be hydrophobic high-molecular-weight compounds existing in human plasma.

Two analyses of the column materials surface demonstrated that the hydrophobic high-molecular-weight compounds in plasma adsorbed onto the surface of the affinity column materials and contributed to the changes in the adsorption ability of plasma protein from immunoaffinity into hydrophobic interactions. Howevere, further studies are needed to characterize the exact details of the compounds.

Conclusions

To investigate the ability to remove abundant proteins from plasma by immnoaffinity using the IgY column, FD-LC-MS/MS method was applied to the long-term test of the reproducibility of the column. It was demonstrated that the immunoaffinity column was effective in removing BSA from the protein standards mixture, but, in addition, removing other proteins in the 18.3–45.0% range. The results suggested that the proteins of possible biomarkers could be lost and their quantification made difficult. Moreover, the specific adsorption of BSA in the protein standards mixture and of albumin in the control human plasma samples decreased with an increase in the number of times the column was used with both samples before its use expired. To examine the cause of the functional changes of the immunoaffinity, the correlations between the adsorption ratio for the affinity column and molecular weight of the adsorbed proteins were calculated, and the column materials surface was also investigated by SEM and

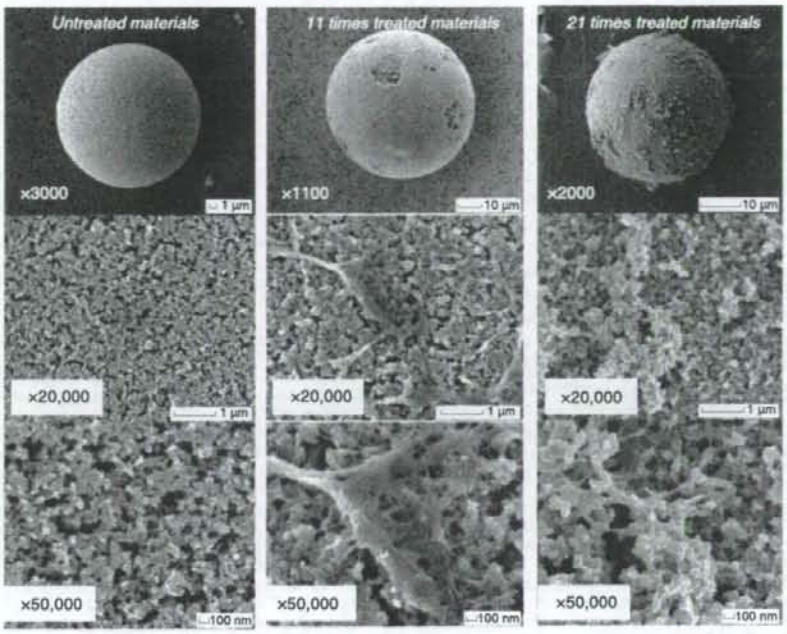

Figure 4. SEM images of the untreated and 11- and 21-times-treated column material surfaces. Magnification in SEM was controlled in a range of × 1100–3000 to show the whole picture of the material.

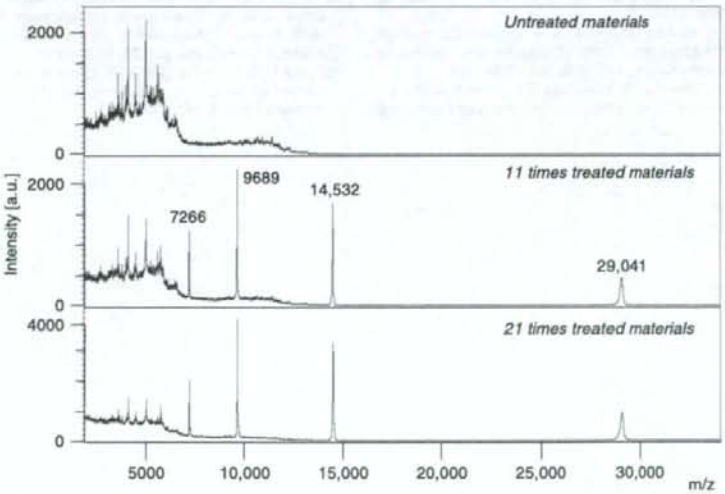

Figure 5. MALDI-TOF-mass spectrum of the untreated and 11- and 21-times-treated column material surface.

MALDI MS analysis. These data demonstrated the attachment of the hydrophobic high-molecular-weight compounds in plasma to the surface, suggesting that on every sample treatment with the affinity column, the adsorption ability of plasma protein changed into hydrophobic interactions. Further studies to characterize the attached compounds are required, and the elucidation of the compounds might lead to the improvement of the affinity column technique and contribute to progress in quantitative plasma proteomics.

Reproducibility is prerequisite for accurate quantitative proteome analysis of clinical samples for biomarker identification and quantification. For this purpose, it is generally essential to

prepare protein samples without high-abundance proteins via specific pre-fractionation techniques to enhance the detection of low-abundance proteins in plasma, and thus, immunoaffinity separation is now chosen as a reliable pre-fractionation method. However, this study indicated that, in quantitative plasma proteomics studies, it is important to keep in mind the risk of not only nonselective loss but also functional changes of the adsorption ability for the immunoaffinity column.

Acknowledgements

We would like to thank Precision System Science Co. Ltd for providing the high-throughput automated proteomic sample processing instrument, Magtration System SA-1, and Bruker Daltonics Japan for performing MALDI MS analysis of the affinity column materials. Part of this work was supported by a MEXT HAITEKU (2004–2008), Grant-in-Aid for Young Scientists (Start-up) and the Mochida Memorial Foundation for Medical and Pharmaceutical Research.

References

Bjorhall K, Miliotis T and Davidsson P. Comparison of different depletion strategies for improved resolution in proteomic analysis of human serum samples. *Proteomics* 2005; **5**: 307–317.

Gong Y, Li X, Yang B, Ying W, Li D, Zhang Y, Dai S, Cai Y, Wang J, He F and Xiaohong Q. Different immunoaffinity fractionation strategies to characterize the human plasma proteome. *Journal of Proteome Research* 2006; **5**: 1379–1387.

Huang L, Harvie G, Feitelson JS, Gramatikoff K, Herold DA, Allen DL, Amunngama R, Hagler RA, Pisano MR, Zhang WW and Xiangming F. Immunoaffinity separation of plasma proteins by IgY microbeads: meeting the needs of proteomic sample preparation and analysis. *Proteomics* 2005; **5**: 3314–3328.

Ichibangase T, Moriya K, Koike K and Imai K. A proteomics method revealing disease-related proteins in livers of hepatitis-infected mouse model. *Journal of Proteome Research* 2007; **6**: 2841–2849.

Ichibangase T, Saimaru H, Takamura N, Kuwahara T, Koyama A, Iwatsubo T and Imai K. Proteomics of Caenorhabditis elegans over-expressing human alpha-synuclein analyzed by fluorogenic derivatization-liquid chromatography/tandem mass spectrometry: identification of actin and several ribosomal proteins as negative markers at early Parkinson's disease stages. *Biomedical Chromatography* 2008; **22**: 232–234.

Imai K, Ichibangase T, Saitoh R and Hoshikawa Y. A proteomics study on human breast cancer cell lines by fluorogenic derivatization–liquid chromatography/tandem mass spectrometry *Biomedical Chromatography* 2008; **22**: 1303–1313.

Linke T, Doraiswamy S and Harrison EH. Rat plasma proteomics: effects of abundant protein depletion on proteomic analysis. *Journal of Chromatography B Analytical Technologies in the Biomedical and Life Dciences* 2007; **849**: 273–281.

Liu T, Qian WJ, Mottaz HM, Gritsenko MA, Norbeck AD, Moore RJ, Purvine SO, Camp DG and Smith RD. Evaluation of multiprotein immunoaffinity subtraction for plasma proteomics and candidate biomarker discovery using mass spectrometry. *Molecular and Cellular Proteomics* 2006; **5**: 2167–2174.

Martosella J, Zolotarjova N, Liu H, Nicol G and Boyes BE. Reversed-phase high-performance liquid chromatographic prefractionation of immunodepleted human serum proteins to enhance mass spectrometry identification of lower-abundant proteins. *Journal of Proteome Research* 2005; **4**: 1522–1537.

Masuda M, Toriumi C, Santa T and Imai K. Fluorogenic derivatization reagents suitable for isolation and identification of cysteine-containing proteins utilizing high-performance liquid chromatography–tandem mass spectrometry. *Analytical Chemistry* 2004; **76**: 728–735.

Plavina T, Wakshull E, Hancock WS and Hincapie M. Combination of abundant protein depletion and multi-lectin affinity chromatography (M-LAC) for plasma protein biomarker discovery. *Journal of Proteome Research* 2007; **6**: 662–671.

Qian WJ, Jacobs JM, Liu T, Camp DG and Smith RD. Advances and challenges in liquid chromatography–mass spectrometry-based proteomics profiling for clinical applications. *Molecular and Cellular Proteomics* 2006; **5**: 1727–1744.

Steel LF, Trotter MG, Nakajima PB, Mattu TS, Gonye G and Block T. Efficient and specific removal of albumin from human serum samples. *Molecular and Cellular Proteomics* 2003; **2**: 262–270.

Toriumi C and Imai K. An identification method for altered proteins in tissues utilizing fluorescence derivatization, liquid chromatography, tandem mass spectrometry, and a database-searching algorithm. *Analytical Chemistry* 2003; **75**: 3725–3730.

Yocum AK, Yu K, Oe T and Blair IA. Effect of immunoaffinity depletion of human serum during proteomic investigations. *Journal of Proteome Research* 2005; **4**: 1722–1731.

J Gastroenterol 2009; 44[Suppl XIX]:82–88
DOI 10.1007/s00535-008-2276-4

Journal of Gastroenterology

Steatosis, liver injury, and hepatocarcinogenesis in hepatitis C viral infection

Kazuhiko Koike

Department of Infectious Diseases, Internal Medicine, Graduate School of Medicine, University of Tokyo, 7-3-1 Hongo, Bunkyo-ku, Tokyo 113-8655, Japan

In addition to the link with development of hepatocellular carcinoma (HCC), hepatitis C virus (HCV) infection is associated with several hepatic and extrahepatic manifestations. A role of hepatic steatosis in the pathogenesis of chronic hepatitis C has been shown, implying hepatitis C as a metabolic disease. Furthermore, recent epidemiological studies have suggested a linkage between insulin resistance and chronic HCV infection. In addition to the data indicating the presence of lipid metabolism disturbance and insulin resistance in the cohort of chronic hepatitis C patients, we found evidence showing the association between these two conditions and HCV infection using mice transgenic for the HCV core gene. These mice develop HCC late in life after the phase of hepatic steatosis and insulin resistance. The nonappearance of both steatosis and HCC in HCV core gene transgenic mice that are null for the proteasome activator 28γ implies a close relationship between lipid metabolism disturbance and hepatocarcinogenesis. Also, the core protein is shown to bind with retinoid X receptor (RXR)-α, resulting in the upregulation of some lipid metabolism enzymes, including cellular retinol binding protein II and acyl-CoA oxidase. In addition, the persistent activation of peroxisome proliferator activated receptor (PPAR)-α has recently been found in the liver of HCV core gene transgenic mice, yielding dramatic changes in lipid metabolism and hepatocyte proliferation, including HCC development. These results would provide a clue for further understanding of the role of lipid metabolism in pathogenesis of HCV infection, including liver injury and hepatocarcinogenesis.

Received: June 9, 2008 / Accepted: August 10, 2008
Reprint requests to: K. Koike

Key words: lipid metabolism, transgenic mouse, oxidative stress, intracellular signal transduction, peroxisome proliferator activated receptor

Introduction

Worldwide, approximately 170 million people are persistently infected with hepatitis C virus (HCV), which induces a spectrum of chronic liver diseases from chronic hepatitis to cirrhosis and, eventually, to hepatocellular carcinoma (HCC).[1] HCV has been given increasing attention because of its wide and deep penetration in the community, tied with a very high incidence of HCC in persistent HCV infection. Once liver cirrhosis is established in hosts persistently infected with HCV, HCC develops at a yearly rate of approximately 7%,[2] resulting in the development of HCC in nearly 90% of HCV-associated cirrhotic patients in 15 years. In addition, the outstanding features in the mode of hepatocarcinogenesis in HCV infection, i.e., development of HCC in a multicentric fashion and at a very high incidence, are not common in other malignancies except for hereditary cancers such as familial polyposis of the colon. Knowledge of the mechanism underlying HCC development in persistent HCV infection, therefore, is imminently required for the prevention of HCC.

In addition to the link with development of HCC, HCV infection is associated with several hepatic and extrahepatic manifestations.[3] A role of hepatic steatosis in the pathogenesis of chronic hepatitis C has been shown, implicating hepatitis C as a metabolic disease.[4] Moreover, recent epidemiological studies have suggested a linkage between insulin resistance and chronic HCV infection.[5] In addition to the epidemiological data indicating the presence of lipid metabolism disturbance and insulin resistance in the cohort of chronic hepatitis C patients, detailed analyses on the relationship between

metabolic disorders and chronic hepatitis C have revealed evidence showing a close association between the progression of liver fibrosis and metabolic abnormalities in HCV infection.[6] However, it is unclear yet whether a causative relationship exists between these medical conditions. Moreover, it is unclear whether such metabolic disorders contribute to hepatocarcinogenesis in HCV infection.

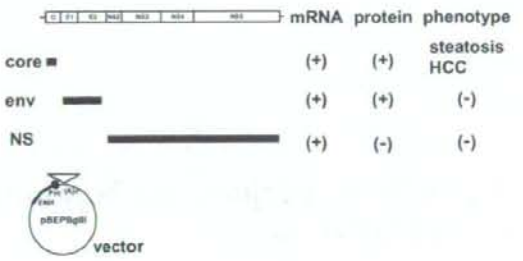

Fig. 1. Transgenic mouse lines carrying the hepatitis C virus (HCV) genome. Three different kinds of transgenic mouse lines, carrying the *core* gene, envelope genes, or nonstructural genes of HCV, respectively, were established under the control of the same regulatory elements. Among these mouse strains, only the transgenic mice carrying the HCV core gene develop hepatocellular carcinoma (HCC) after an early phase with hepatic steatosis in two independent lineages. The mice transgenic for the envelope genes or nonstructural genes do not develop HCC. *HCC*, hepatocellular carcinoma; *env*, envelope genes; *NS*, nonstructural genes

Possible roles of HCV in hepatocarcinogenesis

The mechanism underlying hepatocarcinogenesis in HCV infection is not yet fully understood, despite the fact that nearly 80% of patients with HCC in Japan are persistently infected with HCV.[1,7,8] HCV infection is also common in patients with HCC in other countries, albeit to a lesser extent. These lines of evidence prompted us to seek to determine the role of HCV in hepatocarcinogenesis. Inflammation induced by HCV should be considered, of course, in a study on the hepatocarcinogenesis in hepatitis viral infection: necrosis of hepatocytes caused by chronic inflammation followed by regeneration enhances genetic aberrations in host cells, the accumulation of which culminates in HCC. This theory presupposes an indirect involvement of hepatitis viruses in HCC via hepatic inflammation. However, this context leaves us with a serious question: can inflammation alone result in the development of HCC in such a high incidence (90% in 15 years) or multicentric nature in HCV infection?

The other role of HCV would have to be weighed against an extremely rare occurrence of HCC in patients with autoimmune hepatitis in which severe inflammation in the liver persists indefinitely, even after the development of cirrhosis. This background and reasoning lead to a possible activity of viral proteins for inducing neoplasia. This possibility has been evaluated by introducing genes of HCV into hepatocytes in culture with little success. One of the difficulties in using cultured cells is the carcinogenic capacity of HCV, if any, which would be weak and would take a long time to manifest. Actually, it takes 30–40 years for HCC to develop in individuals infected with HCV. On the basis of these points of view, we started to investigate carcinogenesis in chronic hepatitis C, in vivo, by transgenic mouse technology.

HCV core protein has an in vivo oncogenic activity as revealed by animal studies

Transgenic mouse lines carrying the HCV genome were engineered by introducing the genes from the cDNA of the HCV genome of genotype 1b.[9,10] Established are three different kinds of transgenic mouse lines, which carry the core gene, envelope genes, or nonstructural genes, respectively, under the same transcriptional regulatory element. Among these mouse lines, only the transgenic mice carrying the core gene developed HCC in two independent lineages.[10] The envelope gene transgenic mice do not develop HCC, despite high expression levels of both E1 and E2 proteins,[11,12] and the transgenic mice carrying the entire nonstructural genes have developed no HCC (Fig. 1).

The core gene transgenic mice express the core protein of an expected size, and the level of the core protein in the liver is similar to that in chronic hepatitis C patients. Early in life, these mice develop hepatic steatosis, which is one of the histological characteristics of chronic hepatitis C, along with lymphoid follicle formation and bile duct damage.[13] Thus, the core gene transgenic mouse model reproduces well the features of chronic hepatitis C. Of note, no pictures of significant inflammation are observed in the liver of this animal model. Late in life, these transgenic mice develop HCC. Notably, the development of steatosis and HCC has been reproduced by other HCV transgenic mouse lines, which harbor the entire HCV genome or structural genes including the core gene.[14-16] These outcomes indicate that the core protein, per se, of HCV has an oncogenic potential when expressed in vivo.

Oxidative stress overproduction and intracellular signaling pathway activation are the major pathways in the core-induced liver pathology

It is difficult to elucidate the mechanism underlying the development of HCC, even for our simple model in which only the core protein is expressed in otherwise normal liver. There is a notable feature in the localization of the core protein in hepatocytes; while the core protein predominantly exists in the cytoplasm associated with lipid droplets, it is also present in the mitochondria and nuclei.[10,17] On the basis of this finding, the pathways related to these two organelles, the mitochondria and nuclei, were thoroughly investigated.

One effect of the core protein is an increased production of oxidative stress in the liver. We would like to draw particular attention to the fact that the production of oxidative stress is increased in our transgenic mouse model in the absence of inflammation in the liver. This finding reflects a state of overproduction of reactive oxygen species (ROS) in the liver,[18] or predisposition to it, which is staged by the HCV core protein without any intervening inflammation.[19,20] The overproduction of oxidative stress results in the generation of deletions in mitochondrial and nuclear DNA, an indicator of genetic damage. In addition, analysis of antioxidant system revealed that some antioxidative molecules are not increased despite the overproduction of ROS in the liver of core gene transgenic mice: hemeoxygenase-1 and glutathione peroxidase are not augmented whereas catalase and glutathione S-transferase levels are increased and enhanced by iron overloading (Moriya et al., manuscript in preparation). These results suggest that HCV core protein not only induces overproduction of ROS but also attenuates some of the antioxidant systems, which may explain the mechanism underlying the production of a strong oxidative stress in HCV infection compared to other forms of hepatitis.

In the absence of inflammation, thus, the core protein induces oxidative stress overproduction, which may, at least in part, contribute to hepatocarcinogenesis in HCV infection. If inflammation were added to the liver with the HCV core protein, the production of oxidative stress would be escalated to an extent that can no longer be scavenged by a physiological antagonistic system. This idea suggests that the inflammation in chronic HCV infection would have a characteristic difference in its quality from those of other types of hepatitis, such as autoimmune hepatitis. The basis for the overproduction of oxidative stress may be ascribed to the mitochondrial dysfunction.[10,19] The dysfunction of the electron transfer system of the mitochondrion is suggested in association with the presence of the HCV core protein.[21]

Other pathways in hepatocarcinogenesis would be the alteration of the expression of cellular genes and modulation of intracellular signaling pathways. For example, tumor necrosis factor (TNF)-α and interleukin-1β have been found to be transcriptionally activated.[22] The mitogen-activated protein kinase (MAPK) cascade is also activated in the liver of the core gene transgenic mouse model. The MAPK pathway, which consists of three routes, c-Jun N-terminal kinase (JNK), p38, and extracellular signal-regulated kinase (ERK), is involved in numerous cellular events including cell proliferation. In the liver of the core gene transgenic mouse model before HCC development, only the JNK route is activated. Downstream of JNK activation, transcription factor activating protein (AP)-1 activation is markedly enhanced.[20,21] At far downstream, both the mRNA and protein levels of cyclin D1 and CDK4 are increased. Thus, the HCV core protein modulates the intracellular signaling pathways and gives an advantage for cell proliferation to the hepatocytes. Interestingly, we found recently that a protein interacting with the core protein, proteasome activator 28γ (PA28γ), is indispensable for the core protein to exert its function for the development of steatosis, insulin resistance, and HCC.[23,24]

Lipid metabolism and HCV infection

Steatosis is frequently observed in chronic hepatitis C patients and is significantly associated with increased fibrosis and progression rate of fibrosis of the liver.[6] A comprehensive analysis of gene expression in the liver of core gene transgenic mice, in which steatosis develops from early in life, revealed that a number of genes related to lipid metabolism are significantly upregulated or downregulated (Table 1).

The composition of fatty acids that are accumulated in the liver of core gene transgenic mice is different from that in fatty liver resulting from simple obesity. Carbon-18 monounsaturated fatty acids (C18:1) such as oleic or vaccenic acids are significantly increased; this is also the case in the comparison of liver tissues from hepatitis C patients and patients with simple fatty liver due to obesity.[20] The mechanism of steatogenesis in hepatitis C was investigated using this mouse model. There are at least three pathways for the development of steatosis. One is the frequent presence of insulin resistance in hepatitis C patients as well as in the core gene transgenic mice, which occurs through the inhibition of tyrosine phosphorylation of insulin receptor substrate (IRS)-1.[25] Insulin resistance increases the peripheral release and hepatic uptake of fatty acids, resulting in an accumulation of lipid in the liver. The second pathway is the suppression of the activity of

Table 1. Cellular genes differentially expressed in hepatitis C virus (HCV) core transgenic mouse liver

	Upregulated	Downregulated
Lipid metabolism	NPC1	Stearoyl-CoA desaturase
	Catalase	Sterol-carrier protein X
	Very long chain acyl-CoA dehydrogenase	Alpha-enolase carnitine acetyltransferase
	Carboxylesterase selenoprotein P	Gal beta 1,4(3) GlcNAc alpha 2,3-sialyltransferase
	Carbonic anhydrase	Very long chain acyl-CoA synthetase
	Adipose differentiation-related protein	Liver transferrin
	Bilirubin/phenol family UDP glucuronosyltransferase	4-Hydroxyphenylpyruvate dioxygenase
		LAF1 transketolase
		s-Adenosylmethionine synthetase
		Apolipoprotein A-II
Transcription and cell proliferation	Int-6	Human guanine nucleotide regulatory protein
	GCN5L1	Alpha-fetoprotein
	H. sapiens 8.2k-Da differentiation factor	Retinol binding protein
	USF1	
	Initiation factor eIF-4AI	
	Human elongation factor-1-delta	
	Sui1	
Inflammation	Alpha-1 protease inhibitor 3	Alpha-2-macroglobulin
	Hemopexin	LMW prekininogen
		Complement component C3
		AHSG(alpha 2 HS-glycoprotein) homologue
Others	Microvascular endothelial differentiation gene 1	Vitronectin
	Diazepam-binding inhibitor	Epithelin 1 and 2
	Argininosuccinate synthetase	Murinoglobulin
	Skeletal muscle alpha-tropomyosin	
	Ampd3 gene	
	DNA-binding protein	

microsomal triglyceride transfer protein (MTP) by HCV core protein[26]; this inhibits the secretion of very low density protein (VLDL) from the liver, yielding an increase of triglycerides in the liver. The last pathway involves sterol regulatory element-binding protein (SREBP)-1c, which regulates the production of triglycerides and phospholipids. In HCV core gene transgenic mice, SREBP-1c is activated, whereas neither SREBP-2 nor SREBP-1a is upregulated.[27]

In relation to lipid metabolism, the core protein has also been found to interact with retinoid X receptor (RXR)-α.[28] RXR-α is one of the nuclear receptors, which forms a homodimer or heterodimers with other nuclear receptors, including PPAR (peroxisome proliferator-activated receptor)-α, and plays a pivotal role in the regulation of the expression of genes relating to lipid metabolism, cell differentiation, and proliferation. In fact, the core protein of HCV activates genes that have an RXR-α-responsive element as well as those with a PPAR-α-responsive element, both in mice and in cultured cells.[28] Based on these results, we, then, examined the expression and function of PPAR-α in the liver of core gene transgenic mice.

PPAR-α activation in HCV-associated hepatocarcinogenesis

PPAR-α, one of the PPAR genes, plays a central role as a heterodimer with RXR-α in regulating fatty acid transport and catabolism. It is also known as a molecular target for lipid-lowering fibrate drugs.[29] On the other hand, prolonged administration of PPAR-α agonists causes HCC in rodents. Currently, there is little evidence that the low-affinity fibrate ligands are associated with human cancers, but it is possible that chronic activation of high-affinity ligands could be carcinogenic in humans.[29]

The level of PPAR-α protein was increased in the liver of core gene transgenic mice as early as 9 months of age. PPAR-α protein is accumulated with age in the nuclei of hepatocytes together with cyclin D1 protein. However, the level of PPAR-α mRNA was not increased at any age. By pulse-chase experiment, the stability of nuclear PPAR-α was increased in the presence of the core protein. In line with the increase of PPAR-α protein, target genes of PPAR-α were activated in the liver of core gene transgenic mice; these genes include

cyclin D1, cyclin-dependent kinase (CDK)-4, acy-CoA oxidase, and peroxisome thiolase.[30] However, in general, the activation of PPAR-α leads to improvement but not aggravation of steatosis. Then, what is the function of PPAR-α activation that is observed in the core gene transgenic mice?

To clarify the role of PPAR-α activation in pathogenesis of steatosis and HCC, we mated a core gene transgenic mouse with a PPAR-α knockout (KO) mouse and studied the phenotype. PPAR-α KO mice have reduced expression of target genes of PPAR-α, and have mild steatosis in the liver, as expected.[31] It was unanticipated, however, that steatosis was absent in PPAR-α-null or -heterozygous core gene transgenic mice but present in PPAR-α-intact core gene transgenic mice at the age of 9 or 24 months.[30] 8-Hydroxy deoxyguanosine (8-OHdG) and peroxylipids, both of which are markers for oxidative stress, were decreased in PPAR-α KO core gene transgenic mice. Mitochondrial dysfunction in the core gene transgenic mice, which contributes to overproduction of oxidative stress,[19] was also improved in PPAR-α KO core gene transgenic mice.

Finally, PPAR-α KO core gene transgenic mice did not develop HCC at the age of 24 months, whereas about one-third of PPAR-α-intact core gene transgenic mice did. It should be noted that core gene transgenic mice that are heterozygous for the PPAR-α gene also did not develop HCC.[32] When clofibrate, a peroxisome proliferator, was administered for 24 months to PPAR-α-heterozygous mice, either with or without the core gene, HCC developed in a higher rate in the core gene (+) mice with greater PPAR-α activation. It should be noted that steatosis was present only in core gene (+) PPAR-α-heterozygous mice. In summary, steatosis and HCC developed in PPAR-α-intact but not in PPAR-α-heterozygous or PPAR-α-null core gene transgenic mice, indicating that not the presence but the persistent activation of PPAR-α would be important in hepatocarcinogenesis by HCV core protein. In general, PPAR-α acts to ameliorate steatosis, but with the presence of mitochondrial dysfunction, which is also provoked by the core protein, the core-activated PPAR-α may exacerbate steatosis. Persistent activation of PPAR-α with "strong" ligands such as the core protein of HCV could be carcinogenic in humans, although the low-affinity fibrate ligands are not likely associated with human cancers.

HCV core protein causes "fatty acid spiral"

Figure 2 illustrates our current hypothesis for the role of lipid metabolism in HCV-associated hepatocarcinogenesis. Immune-mediated inflammation should also play a pivotal role in hepatocarcinogenesis in HCV infection. However, in HCV infection, the core protein induces steatosis through the aforementioned pathways, leading to "fatty acid spiral" in the presence of the mitochondrial complex 1 dysfunction and PPAR-α activation, both of which are caused by the core protein. These intracellular alterations would contribute to hepatocarcinogenesis by inducing oxidative stress overproduction and cell-growth signal activation. In such a sense, the core protein of HCV is not a classical-type oncoprotein, but rather seems to contribute to hepatocarcinogenesis by modulating intracellular metabolism and signaling.

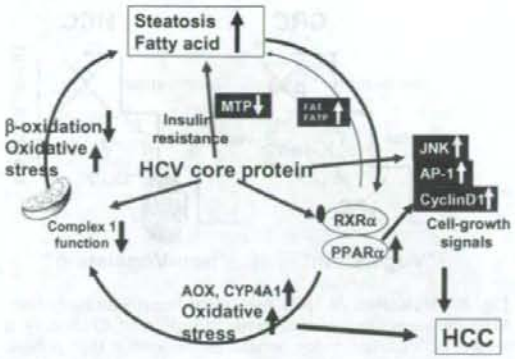

Fig. 2. "Fatty acid spiral" by HCV core protein. In HCV infection, the core protein induces steatosis via several pathways, leading to "fatty acid spiral" in the presence of the mitochondrial complex 1 dysfunction and PPAR-α activation, both of which are also caused by the core protein. These intracellular alterations would contribute to hepatocarcinogenesis by inducing oxidative stress overproduction and cell-growth signal activation. In such a sense, the core protein of HCV is not a classical type oncoprotein, but rather seems to contribute to hepatocarcinogenesis by modulating intracellular metabolism and signaling. *HCV*, hepatitis C virus; *HCC*, hepatocellular carcinoma; *ROS*, reactive oxygen species; *JNK*, c-Jun N-terminal kinase; *ERK*, extracellular signal-regulated kinase; *AP-1*, activating protein-1; *RXR-α*, retinoid X receptor-α; *PPAR-α*, peroxisome proliferator activated receptor-α; *AOX*, acyl-CoA oxidase; *CYP*, cytochrome P450; *MTP*, microsomal triglyceride transfer protein; *FAT*, fatty acid translocase; fatty acid transport protein

The HCV protein may allow some steps in multistep hepatocarcinogenesis to be skipped

The results of our studies on transgenic mice have indicated a carcinogenic potential of the HCV core protein in vivo; thus, HCV would be directly involved in hepatocarcinogenesis. In research studies of carcinogenesis, the theory outlined by Kinzler and Vogelstein[33] has gained wide popularity. They have proposed that the

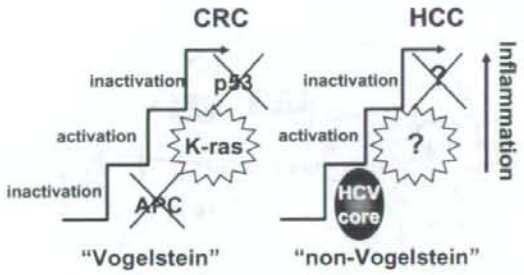

Fig. 3. Mechanism of HCV-associated hepatocarcinogenesis. Multiple steps are required in the induction of all cancers; it would be mandatory for hepatocarcinogenesis that genetic mutations accumulate in hepatocytes. However, in HCV infection, some of these steps may be skipped in the development of HCC in the presence of the core protein. The overall effects achieved by the expression of the core protein would be the induction of HCC, even in the absence of a complete set of genetic aberrations required for carcinogenesis. By considering such a "non-Vogelstein-type" process for the induction of HCC, a plausible explanation may be given for many unusual events happening in HCV carriers

development of colorectal cancer is induced by the accumulation of a complete set of cellular gene mutations. They have deduced that mutations in the APC gene for inactivation, those in K-*ras* for activation, and those in the p53 gene for inactivation accumulate, which cooperate toward the development of colorectal cancer.[33] Their theory has been extended to the carcinogenesis of other cancers as well, called "Vogelstein-type" carcinogenesis (Fig. 3).

On the basis of the results we obtained for the induction of HCC by the HCV core protein, we would like to introduce a different mechanism for hepatocarcinogenesis in HCV infection. We do allow multistages in the induction of all cancers; it would be mandatory for hepatocarcinogenesis that many mutations accumulate in hepatocytes. Some of these steps, however, may be skipped in the development of HCC in HCV infection to which the core protein would contribute (see Fig. 3). The overall effect achieved by the expression of the viral protein would be the induction of HCC, even in the absence of a complete set of genetic aberrations required for carcinogenesis.

By considering such a "non-Vogelstein-type" process for the induction of HCC, a plausible explanation may be given for many unusual events happening in HCV carriers.[34] Now it does not seem so difficult as before to determine why HCC develops in persistent HCV infection at an outstandingly high incidence. Our theory may also give an account of the nonmetastatic and multicentric de novo occurrence characteristics of HCC, which would be the result of persistent HCV infection.

References

1. Saito I, Miyamura T, Ohbayashi A, Harada H, Katayama T, Kikuchi S, et al. Hepatitis C virus infection is associated with the development of hepatocellular carcinoma. Proc Natl Acad Sci USA 1990;87:6547–9.
2. Ikeda K, Saitoh S, Suzuki Y, Kobayashi M, Tsubota A, Koida I, et al. Disease progression and hepatocellular carcinogenesis in patients with chronic viral hepatitis: a prospective observation of 2215 patients. J Hepatol 1998;28:930–8.
3. Okuse C, Yotsuyanagi H, Koike K. Hepatitis C as a systemic disease: virus and host immunologic responses underlie hepatic and extrahepatic manifestations. J Gastroenterol 2007;42:857–65.
4. Koike K, Moriya K. Metabolic aspects of hepatitis C: steatohepatitis distinct from NASH. J Gastroenterol 2005;40:329–36.
5. Negro F. Insulin resistance and HCV: will new knowledge modify clinical management? J Hepatol 2006;45:514–9.
6. Powell EE, Jonsson JR, Clouston AD. Steatosis: co-factor in other liver diseases. Hepatology 2005;42:5–13.
7. Kiyosawa K, Sodeyama T, Tanaka E, Gibo Y, Yoshizawa K, Nakano Y, et al. Interrelationship of blood transfusion, non-A, non-B hepatitis and hepatocellular carcinoma: analysis by detection of antibody to hepatitis C virus. Hepatology 1990;12:671–5.
8. Yotsuyanagi H, Shintani Y, Moriya K, Fujie H, Tsutsumi T, Kato T, et al. Virological analysis of non-B, non-C hepatocellular carcinoma in Japan: frequent involvement of hepatitis B virus. J Infect Dis 2000;181:1920–8.
9. Moriya K, Yotsuyanagi H, Shintani Y, Fujie H, Ishibashi K, Matsuura Y, et al. Hepatitis C virus core protein induces hepatic steatosis in transgenic mice. J Gen Virol 1997;78:1527–31.
10. Moriya K, Fujie H, Shintani Y, Yotsuyanagi H, Tsutsumi T, Matsuura Y, et al. Hepatitis C virus core protein induces hepatocellular carcinoma in transgenic mice. Nat Med 1998;4:1065–8.
11. Koike K, Moriya K, Ishibashi K, Matsuura Y, Suzuki T, Saito I, et al. Expression of hepatitis C virus envelope proteins in transgenic mice. J Gen Virol 1995;76:3031–8.
12. Koike K, Moriya K, Yotsuyanagi H, Shintani Y, Fujie H, Ishibashi K, et al. Sialadenitis resembling Sjögren's syndrome in mice transgenic for hepatitis C virus envelope genes. Proc Natl Acad Sci USA 1997;94:233–6.
13. Bach N, Thung SN, Schaffner F. The histological features of chronic hepatitis C and autoimmune chronic hepatitis: a comparative analysis. Hepatology 1992;15:572–7.
14. Lerat H, Honda M, Beard MR, Loesch K, Sun J, Yang Y, et al. Steatosis and liver cancer in transgenic mice expressing the structural and nonstructural proteins of hepatitis C virus. Gastroenterology 2002;122:352–65.
15. Naas T, Ghorbani M, Alvarez-Maya I, Lapner M, Kothary R, De Repentigny Y, et al. Characterization of liver histopathology in a transgenic mouse model expressing genotype 1a hepatitis C virus core and envelope proteins 1 and 2. J Gen Virol 2005;86:2185–96.
16. Machida K, Cheng KT, Lai CK, Jeng KS, Sung VM, Lai MM. Hepatitis C virus triggers mitochondrial permeability transition with production of reactive oxygen species, leading to DNA damage and STAT3 activation. J Virol 2006;80:7199–207.
17. Moriya K, Fujie H, Yotsuyanagi H, Shintani Y, Tsutsumi T, Matsuura Y, et al. Subcellular localization of hepatitis C virus structural proteins expressed in transgenic liver. Jpn J Med Sci Biol 1997;50:169–77.
18. Sasaki Y. Does oxidative stress participate in the development of hepatocellular carcinoma? J Gastroenterol 2006;41:1135–48.
19. Moriya K, Nakagawa K, Santa T, Shintani Y, Fujie H, Miyoshi H, et al. Oxidative stress in the absence of inflammation in a mouse model for hepatitis C virus-associated hepatocellular carcinogenesis. Cancer Res 2001;61:4365–70.

20. Moriya K, Todoroki T, Tsutsumi T, Fujie H, Shintani Y, Miyoshi H, et al. Increase in the concentration of carbon 18 monounsaturated fatty acids in the liver with hepatitis C: analysis in transgenic mice and humans. Biophys Biochem Res Commun 2001;281: 1207–12.
21. Okuda M, Li K, Beard MR, Showalter LA, Scholle F, Lemon SM, Weinman SA. Mitochondrial injury, oxidative stress, and antioxidant gene expression are induced by hepatitis C virus core protein. Gastroenterology 2002;122:366–75.
22. Tsutsumi T, Suzuki T, Moriya K, Yotsuyanagi H, Shintani Y, Fujie H, et al. Intrahepatic cytokine expression and AP-1 activation in mice transgenic for hepatitis C virus core protein. Virology 2002;304:415–24.
23. Tsutsumi T, Suzuki T, Moriya K, Shintani Y, Fujie H, Miyoshi H, et al. Hepatitis C virus core protein activates ERK and p38 MAPK in cooperation with ethanol in transgenic mice. Hepatology 2003;38:820–8.
24. Miyamoto H, Moriishi K, Moriya K, Murata S, Tanaka K, Suzuki T, et al. Hepatitis C virus core protein induces insulin resistance through a PA28γ-dependent pathway. J Virol 2007;81:1727–35.
25. Shintani Y, Fujie H, Miyoshi H, Tsutsumi T, Kimura S, Moriya K, et al. Hepatitis C virus and diabetes: direct involvement of the virus in the development of insulin resistance. Gastroenterology 2004;126:840–8.
26. Perlemuter G, Sabile A, Letteron P, Vona G, Topilco A, Koike K, et al. Hepatitis C virus core protein inhibits microsomal triglyceride transfer protein activity and very low density lipoprotein secretion: a model of viral-related steatosis. FASEB J 2002; 16:185–94.
27. Moriishi K, Mochizuki R, Moriya K, Miyamoto H, Mori Y, Abe T, et al. Critical role of PA28γ in hepatitis C virus-associated steatogenesis and hepatocarcinogenesis. Proc Natl Acad Sci USA 2007;104:1661–6.
28. Tsutsumi T, Suzuki T, Shimoike T, Moriya K, Yotsuyanagi H, Matsuura Y, et al. Interaction of hepatitis C virus core protein with retinoid X receptor-α modulates its transcriptional activity. Hepatology 2002;35:937–46.
29. Peters JM, Cheung C, Gonzalez FJ. Peroxisome proliferator-activated receptor-alpha and liver cancer: where do we stand? J Mol Med 2005;83:774–85.
30. Tanaka N, Moriya K, Kiyosawa K, Koike K, Aoyama T. Hepatitis C virus core protein induces spontaneous and persistent activation of peroxisome proliferator-activated receptor alpha in transgenic mice: implications for HCV-associated hepatocarcinogenesis. Int J Cancer 2008;122:124–31.
31. Akiyama TE, Sakai S, Lambert G, Nicol CJ, Matsusue K, Pimprale S, et al. Conditional disruption of the peroxisome proliferator-activated receptor gamma gene in mice results in lowered expression of ABCA1, ABCG1, and apoE in macrophages and reduced cholesterol efflux. Mol Cell Biol 2002;22: 2607–19.
32. Tanaka N, Moriya K, Kiyosawa K, Koike K, Gonzalez FJ, Aoyama T. PPAR-α is essential for severe hepatic steatosis and hepatocellular carcinoma induced by HCV core protein. J Clin Invest 2008;118:683–94.
33. Kinzler KW, Vogelstein B. Lessons from hereditary colorectal cancer. Cell 1996;87:159–70.
34. Koike K. Molecular basis of hepatitis C virus-associated hepatocarcinogenesis: lessons from animal model studies. Clin Gastroenterol Hepatol 2005;3:S132–5.

THE JOURNAL OF BIOLOGICAL CHEMISTRY VOL. 284, NO. 6, pp. 3513–3520, February 6, 2009

A Single Amino Acid of Toll-like Receptor 4 That Is Pivotal for Its Signal Transduction and Subcellular Localization*

Received for publication, April 22, 2008, and in revised form, October 29, 2008 Published, JBC Papers in Press, December 8, 2008, DOI 10.1074/jbc.M803086200

Shintaro Yanagimoto[‡§¶], Keita Tatsuno[§], Shu Okugawa[§], Takatoshi Kitazawa[§], Kunihisa Tsukada[§], Kazuhiko Koike[§], Tatsuhiko Kodama[¶], Satoshi Kimura[‖], Yoshikazu Shibasaki[‡1], and Yasuo Ota[1,2]**

From the [‡]Center for Structuring Life Sciences, Graduate school of Arts and Sciences, University of Tokyo, Meguro-ku, Tokyo 153-8903, the [§]Department of Infectious Diseases, Graduate School of Medicine, University of Tokyo, Bunkyo-ku, Tokyo 113-8655, the [¶]Laboratory for Systems Biology and Medicine, Research Center for Advanced Science and Technology, University of Tokyo, Meguro-ku, Tokyo 153-8904, the [‖]Tokyo Teishin Hospital, Fujimi, Chiyoda-ku, Tokyo 102-8798, and the [**]Department of Medicine, Teikyo University School of Medicine, 2-11-1, Kaga, Itabashi-ku, Tokyo 173-8605, Japan

Toll-like receptor 4 (TLR4) is essential for recognizing a Gram-negative bacterial component, lipopolysaccharide (LPS). A single amino acid mutation at position 712 of murine TLR4 leads to hyporesponsiveness to LPS. In this study we determined that an amino acid, a leucine at position 815 of human TLR4, is also pivotal for LPS responsiveness and subcellular distribution. By replacing the leucine with alanine, the mutant TLR4 lost responsiveness to LPS and did not localize on the plasma membrane. In addition, it does not coprecipitate with myeloid differentiation-2, an accessory protein that is necessary for TLR4 to recognize LPS. These results suggest that the leucine at position 815 is required for the normal maturation of TLR4 and for formation of the TLR4·MD-2 complex.

Toll-like receptors (TLRs)[3] play essential roles in both innate and adaptive immunity (1). Thirteen members of the TLR family have been identified in mammals. TLRs have leucine-rich-repeats in their extracellular domains and a Toll/Interleukin-1 receptor (TIR) in their cytoplasmic domains, the latter of which mainly mediates intracellular signaling. Signaling pathways of TLRs, except for TLR3, depend on an adapter protein, MyD88 (myeloid differentiation factor 88), which interacts with the TIR domain of TLRs. This pathway leads to the activation of the transcription factor NF-κB and production of cytokines such as tumor necrosis factor-α and interleukin-6. Another important signaling pathway mediated by TLR3 and TLR4 that exploits the TIR domain is the MyD88-independent pathway. This pathway involves different adapter proteins, such as the TIR domain-containing adaptor inducing interferon-β (TRIF) and TRIF-related adaptor molecule (2–4), and is essential for production of type I interferon through activation of interferon regulatory factor-3.

TLRs recognize as ligands several microbial pathogen-associated molecular patterns. One such pathogen-associated molecular pattern is lipopolysaccharide (LPS), which is recognized by TLR4. LPS triggers severe immunologic reactions by the host in Gram-negative bacterial infections and has drawn attention in many clinical situations. TLR4 is the first mammalian TLR to be discovered in the context of immunology. TLR4 was identified in the search for the genes responsible for LPS hyporesponsiveness (5, 6). The defect was found to stem from a single amino acid mutation, replacement of proline with histidine at position 712, in the cytoplasmic tail of murine TLR4. The study led to the discovery of the importance of TLR4 in innate immunity.

A variety of cells are activated by LPS stimulation through TLR4. TLR4 forms a receptor complex with an accessory protein, myeloid differentiation-2 (MD-2). MD-2 first associates with TLR4 in the endoplasmic reticulum (ER) and *cis*-Golgi, and both proteins move together to the plasma membrane (7, 8). Upon recognition of LPS, the TLR4·MD-2 complex receives LPS on the cell surface and initiates intracellular signaling. The expression of TLR4 in the absence of MD-2 does not confer full responsiveness to LPS stimuli in experimental cell lines (9). An analysis of MD-2 knockout mice revealed that MD-2 is important not only for LPS sensing but also for cellular distribution of TLR4.

In this study we hypothesized that the cytoplasmic tail of TLR4 contains regions that control both localization and signaling. Using truncation and mutation analysis, and paying particular attention to the TIR domain, we identified a single amino acid that is pivotal for both TLR4 signaling and subcellular distribution. The site we found was on the C-terminal portion of the TIR domain for which no specific function has been yet determined.

* This work was partly supported by the Program of Fundamental Studies in Health Sciences of the National Institute of Biomedical Innovation, by the Focus 21 project of the New Energy and Industrial Technology Development Organization, and by the Special Coordination Fund for Science and Technology from the Ministry of Education, Culture, Sports, Science and Technology. This study was also partly supported by a grant-in-aid from the Ministry of Education, Culture, Sports, Science and Technology (to Y. O.). The costs of publication of this article were defrayed in part by the payment of page charges. This article must therefore be hereby marked "*advertisement*" in accordance with 18 U.S.C. Section 1734 solely to indicate this fact.

[1] Both authors contributed equally to this work.

[2] To whom correspondence should be addressed. Tel.: 81-3-3964-1211 (ext. 1756); Fax: 81-3-3579-6310; E-mail: yasuota-tky@umin.ac.jp.

[3] The abbreviations used are: TLR, Toll-like receptor; TIR, Toll/Interleukin-1 receptor; TRIF, TIR domain-containing adaptor inducing interferon-β; LPS, lipopolysaccharide; MD-2, myeloid differentiation-2; ER, endoplasmic reticulum; GFP, green fluorescent protein; EGFP, enhanced GFP; RLA, relative luciferase activity; Sulfo-NHS-SS-Biotin, sulfosuccinimidyl-2-(biotinamido)ethyl-1,3-dithiopropionate.

EXPERIMENTAL PROCEDURES

Reagents and Other Materials—Lipopolysaccharide (LPS) from *Escherichia coli* O55:B5 was purchased from Sigma-Aldrich and applied without repurification. FLAG- and hexa-histidine (His_6)-tagged human TLR4 expression plasmid (pEFBOS/humanTLR4flaghis) and FLAG- and His_6-tagged human MD-2 expression plasmid (pEFBOS/humanMD-2flaghis) were generous gifts from Dr. Kensuke Miyake (Institute of Medical Science, University of Tokyo, Japan). Human CD14 cDNA plasmid (pCMV6-XL5/humanCD14) was purchased from OriGene (Rockville, MD). Fluorescent protein expression vector pEGFP-N3 was purchased from Clontech (Mountain View, CA). Anti-TLR4 monoclonal antibody (clone HTA125) was purchased from Abcam (Cambridge, MA). Anti-FLAG monoclonal antibody (clone M2) was purchased from Sigma-Aldrich. Anti-*A.v.* (GFP) monoclonal and polyclonal antibodies were purchased from Clontech. Control immunoglobulins for immunoprecipitation were purchased from BD Biosciences (San Jose, CA). Horseradish peroxidase-labeled anti-immunoglobulins antibodies were purchased from Dako (Glostrup, Denmark). BlockAce (DS Pharma Biomedical, Osaka, Japan) solution was used as blocking buffer for Western blotting.

Cell Culture—Human embryonic kidney (HEK) 293T cells were maintained in Dulbecco's modified Eagle's medium (Sigma-Aldrich) containing 10% heat-inactivated fetal bovine serum supplemented with penicillin-streptomycin solution (Invitrogen). FuGENE 6 transfection reagent (Roche Applied Science) was used for transient cotransfection according to the manufacturer's instructions. Culture dishes or plates were prepared to 70% confluence prior to transfection. Cells were used for experiments 36 h later. The transfection conditions were optimized for microscopic observation of the expressed fluorescent protein and were kept unchanged in other experiments.

Expression Vector Subcloning and Mutagenesis—Wild-type TLR4 cDNA was excised from pEFBOS/humanTLR4flaghis and subcloned into pEGFP-N3 so that when expressed enhanced green fluorescent protein (EGFP) would be fused at the C terminus of TLR4 (pEGFP-N3/humanTLR4). All mutations were introduced into pEFBOS/humanTLR4flaghis and pEGFP-N3/humanTLR4 using the QuikChange site-Directed mutagenesis kit (Stratagene, La Jolla, CA) according to the manufacturer's instructions and were confirmed by sequencing. For the truncation analysis, two identical unique restriction sites were prepared in the TLR4-coding region of pEFBOS/humanTLR4 using a QuikChange kit, and the DNA fragment to be removed, which was a part of the C terminus of TLR4, was excised enzymatically. After agarose gel purification, the linear double-stranded DNA was ligated to re-form a circular plasmid. Restriction sites were designed so as not to cause a frameshift between TLR4 and EGFP.

Confocal Laser Scanning Microscopy of Cells—Samples were fixed in 3% paraformaldehyde-phosphate-buffered saline at 37 °C for 10 min. Fluorescence images of fixed samples were recorded using a FluoView FV1000 Confocal Microscope (an inverted confocal laser scanning microscope, Olympus, Tokyo, Japan).

Immunoprecipitation—Transfected cells were lysed in lysis buffer (50 mM Tris-HCl, pH 7.5, 100 mM NaCl, 0.1% Triton X-100, 1 mM 1,4-dithiothreitol, and proteinase inhibitor mixture), sonicated, and centrifuged at 4 °C. Antibody was added to the supernatant, and the sample was rotated 1 h at 4 °C followed by the addition of protein G-Sepharose (GE Healthcare Life Sciences, Piscataway, NJ) and an additional 8-h incubation at 4 °C. Bound protein was washed three times in lysis buffer. Proteins were eluted by boiling in SDS sample buffer.

Biotinylation and Purification of Cell Surface Proteins—Prior to surface biotinylation, HEK 293T cells plated in a 100-mm dish were transiently transfected as described above. Surface biotinylation and subsequent purification of biotinylated proteins were performed using a Cell Surface Protein Biotinylation and Purification Kit (Pierce) following the manufacturer's instructions. Briefly, membrane-impermeable sulfosuccinimidyl-2-(biotinamido)ethyl-1,3-dithiopropionate (Sulfo-NHS-SS-Biotin) was added to cell monolayers in the culture dishes and covalently bound to amines in proteins exposed on the cell surface. The affinity resin that binds to the biotin end of Sulfo-NHS-SS-Biotin was used to collect the biotinylated proteins. Reduction by 1,4-dithiothreitol causes cleavage of the disulfide bond in Sulfo-NHS-SS-Biotin, and the elute contains the biotinylated cell surface proteins. Each final sample obtained was considered to contain proteins from an equal amount of cells, because all culture plates were treated equally and grown to full confluence. All samples were sonicated and subjected to SDS-PAGE and Western blotting. The membrane to which protein was transferred was blocked in blocking buffer for 1 h. Then the membrane was incubated with a primary antibody, followed by incubation with horseradish peroxidase-labeled anti-immunoglobulins antibody. The protein bands were then visualized by using a chemiluminescence reagent, Immobilon Western Chemiluminescent HRP Substrate (Millipore, Billerica, MA), according to the manufacturer's instructions.

Cell Stimulation Assays—HEK293T cells were plated and transiently transfected for assays. Thirty-six hours after the transfection, LPS was added to fresh culture medium in each well of the culture plates at the stated concentration. The duration of LPS stimulation was 7 h.

Dual Luciferase Reporter Assays for NF-κB Activation—HEK293T cells were plated in 12-well culture plates (4×10^4 cells/well), and experimental cDNA plasmids were transiently transfected 36 h later using the FuGENE 6 transfection reagent with 0.5 μg of NF-κB reporter plasmid expressing firefly luciferase (pNF-κB-Luc, Stratagene) and 0.05 μg of constitutively active *Renilla* luciferase reporter plasmid (pRL-TK, Promega, Madison, WI) in addition to 0.5 μg each of TLR4-EGFP plasmid and MD-2 plasmid. Stimulation experiments were performed 36 h later. Firefly luciferase and *Renilla* luciferase activities were measured using the Dual-Luciferase Reporter Assay System (Promega) and the Genelight55 luminometer (Microtech, Chiba, Japan). Relative luciferase activity (RLA) was obtained as the ratio of firefly luciferase activity to *Renilla* luciferase activity. Results are expressed as the ratio of RLA with LPS stimulation to RLA without LPS stimulation ([RLA LPS+]/[RLA LPS−]). This ratio should ideally approach 1 when no response to LPS stimulation is observed.

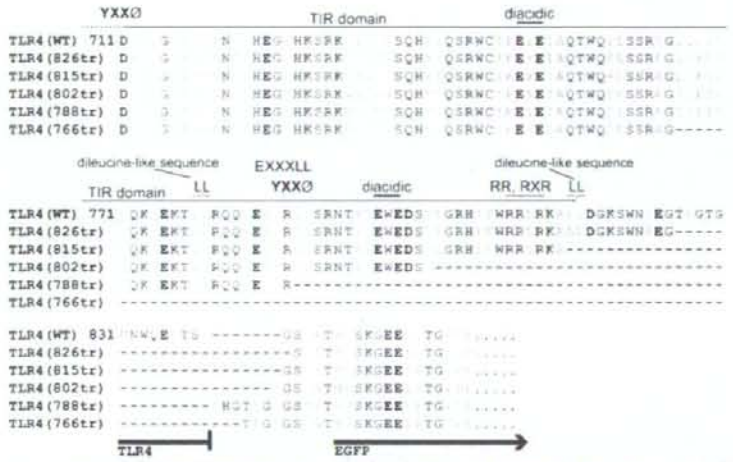

FIGURE 1. **Alignment of the cytoplasmic domains of EGFP fusion TLR4 truncation mutants used in this study.** TLR4 (766tr) signifies the mutant truncated at position 766. Others are named in the same manner. The amino acids are colored based on their physicochemical properties: *pink*, basic; *blue*, acidic; *green*, polar and neutral; and *orange*, hydrophobic. The *black overline* represents the TIR domain. *Colored overlines* indicate amino acid sequences identical to known sorting signal motifs except for two LLs, which are dileucine motif-like sequences in that they consist of solely two consecutive leucines without preceding aspartate or glutamate. *Capital letters* on the *line* signify the single-letter code for amino acids: *E*, glutamic acid; *L*, leucine; *R*, arginine; and *Y*, tyrosine. *X* signifies any amino acid, and Ø signifies an amino acid residue with a bulky hydrophobic side chain.

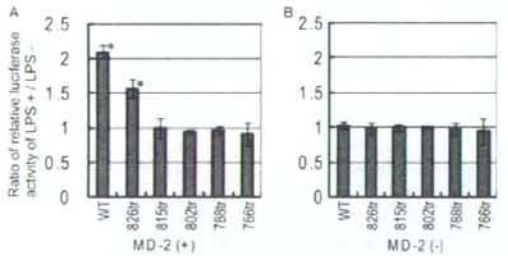

FIGURE 2. **LPS responsiveness measured by NF-κB luciferase assay.** HEK293T cells were transfected with plasmids containing the gene for wild-type TLR4 or a truncated human TLR4-EGFP fusion protein, in addition to a luciferase reporter and human MD-2 plasmid (*A*) or unmodified plasmids (control) (*B*). After 36 h, cells were stimulated with LPS (10 ng/ml) for 7 h, and luciferase reporter gene activity was measured. All results were expressed as the ratio of relative luciferase activity with LPS stimulation to that without stimulation. The data were from three independent experiments. *Small bars* indicate 95% confidence intervals of the mean (*p* values for * are: TLR4 (WT)-EGFP/MD-2 (+), $p = 0.002$; TLR4 (826tr)-EGFP/MD-2 (+), $p = 0.016$).

Statistical Analyses—All quantitative experiments were repeated three times, and each experiment was done in triplicate. The ratio of relative luciferase activity of LPS+ to LPS− was calculated as the index of the responsiveness to the stimuli as explained above. When positive response is observed, the ratio should significantly exceed one. The means of the ratio were represented in *bar graphs*. The 95% confidence interval of the mean of the ratio was calculated and indicated on each *bar* in the *graph*, and *p* values were calculated using Student's *t* distribution compared with the hypothetical mean, one.

RESULTS

Truncation Analysis of TLR 4—To identify amino acid sequences in the cytoplasmic tail of TLR4 that are involved in both signal transduction and subcellular distribution, first we generated five truncation mutants of TLR4 with a fluorescent protein (EGFP) at the C terminus of TLR4.

Although there are no known definite sorting signal motifs in the cytoplasmic tail of TLR4, some amino acid sequences are similar or identical to known general sorting signal motifs as shown in Fig. 1. *YXXØ*, a form of tyrosine-based sorting signal, and *EXXXLL*, a form of dileucine (LL)-based sorting signal, both control protein internalization, lysosomal targeting, and basolateral targeting (10), where "*X*" represents any amino acid, "*Ø*" stands for an amino acid residue with a bulky hydrophobic side chain, and other letters are single-letter abbreviations for the amino acids. "Diacidic" signals such as *DXE* mediate export from the ER (11). RR or *RXR* is another example of an ER export signal (12). Truncation sites were chosen so that some of these amino acid sequences were deleted in each mutant. Because the TIR domain, which is essential in TLR4 signaling and possibly subcellular localization (13), spans most of the cytoplasmic domain of TLR4, four out of five mutants have involvement in the TIR domain, which we hypothesized could result in impaired signal transduction and a change in subcellular distribution. Part of the cytoplasmic portion of the amino acid sequence of the truncation mutants is shown in Fig. 1. The five truncation mutant proteins lost their C-terminal tails at positions 826, 815, 802, 788, and 766, respectively, and were conjugated with EGFP *in vitro*. Actual truncation and ligation sites of all actual mutants were confirmed to have the designed DNA alignment by sequencing.

We utilized the luciferase reporter assay to assess NF-κB transcription activity as an indicator of TLR4 response to LPS stimuli. MD-2 is reported to be essential for this response (9). However, because it is not known whether MD-2 is necessary for transduction of the truncated TLR4 signal as well, we performed the assays with and without MD-2. The index of cell responsiveness to the stimulation was measured as the ratio between RLA with LPS stimulation and RLA without LPS stimulation. Only cells transfected with TLR4 (826tr)-EGFP in combination with MD-2 retained responsiveness to LPS stimulation. One exception was wild-type TLR4-EGFP (Fig. 2*A*). HEK293T cells transfected with TLR4 but without MD-2 did not respond to LPS stimuli regardless of the TLR4-EGFP genotype (Fig. 2*B*).

Next, we compared the localization of wild-type and truncated mutants of TLR4-EGFP in HEK293T by fluorescence microscopy (Fig. 3*A*). The wild-type TLR4 cotransfected with MD-2 was expressed on the plasma membrane and also in the

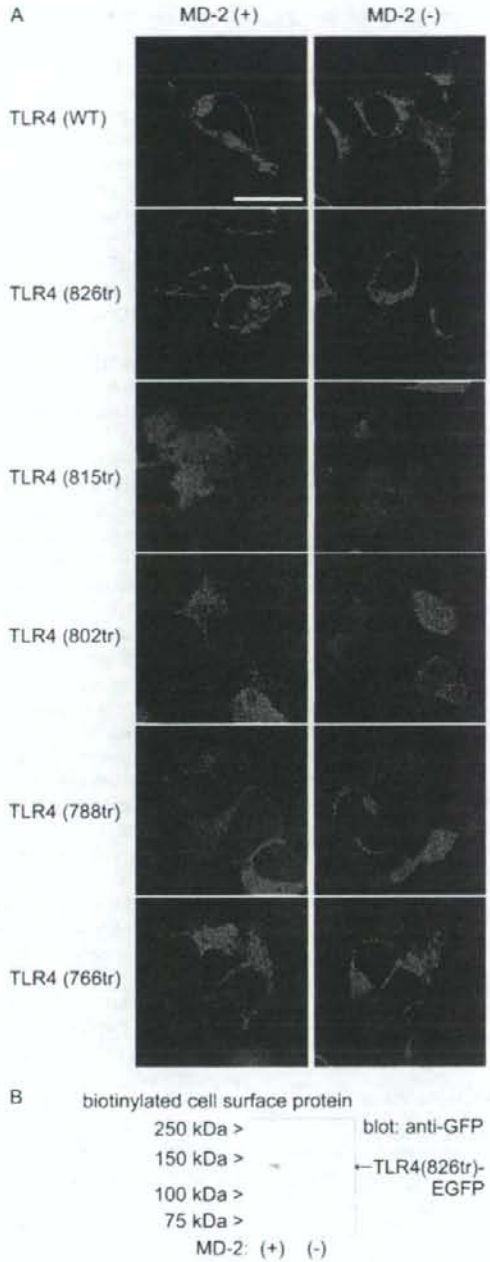

FIGURE 3. **Residues 815–826 of TLR4 contain a region necessary for plasma membrane localization.** *A*, cells were cultured on coverslips in 12-well plates and transfected as in Fig. 2. EGFP-tagged TLR4 was visualized by laser confocal microscopy. Fluorescence from EGFP was observed in *green*. Each genotype of TLR4-EGFP was cotransfected with a human MD-2 plasmid or empty vector. *Bar*, 20 μm. *B*, TLR4 (826tr)-EGFP with or without coexpression of MD-2 were tagged by biotinylation of the cell surface proteins and affinity-purified. TLR4 was visualized by immunoblotting using an anti-GFP monoclonal antibody. Samples from both combinations of DNAs were prepared from the same number of cells.

perinuclear area. These findings were consistent with observations by others (14, 15). TLR4 is reported to localize in the Golgi apparatus as well as on the plasma membrane. Our observation of TLR4-EGFP accumulation in the perinuclear area does not contradict the report that TLR4 partly localizes in the Golgi apparatus (14).

TLR4-EGFP truncation mutants, 815tr, 802tr, 788tr, and 766tr apparently did not localize at the plasma membrane. No particular fluorescence pattern that might be characteristic of localization to a specific intracellular compartment was observed. Only TLR4 (826tr)-EGFP, which has the shortest truncation, was expressed on the plasma membrane and in the perinuclear area, and the fluorescence pattern was similar to that of wild-type (Fig. 3*A*). No TLR4 genotypes, including wild-type TLR4-EGFP, clearly localized on the plasma membrane in the absence of MD-2 (Fig. 3*A*). MD-2 is reported to be necessary for localization of wild-type TLR4 at the plasma membrane (15), which is consistent with our observation. Intracellular distribution of mutant TLR4 varied depending on the genotype, but no particular cellular structure was identified as an alternative target site. Furthermore, we examined the plasma membrane expression of TLR4 (826tr)-EGFP by cell surface protein biotinylation. The expression level of TLR4 (826tr)-EGFP was markedly decreased without coexpression of MD-2 (Fig. 3*B*), which is compatible with the microscope observation.

Removal of the C-terminal segment of TLR4 at residue 826 does not qualitatively affect LPS responsiveness and subcellular distribution. However, when more residues, up to position 815, were removed, both signal transduction and plasma membrane localization were impaired. These results suggest that residues 815–826 of TLR4 contain at least one segment that is critical for those functions.

Amino Acid Sequence Replacement Analysis—To identify critical amino acid sequences in this region, we generated an amino acid replacement mutant of TLR4 instead of truncation mutants. As shown in Fig. 1, although it is not a canonical sequence, leucine-leucine at 815–816 partially fits a known sorting signal motif, a dileucine motif, (D/E)*XXX*L(L/I) or D*XX*LL, which plays an important role in internalization of plasma membrane protein or sorting from the *trans*-Golgi network (10). Thus, as has been done in a similar study (16), a mutant was generated in which alanines were substituted for both leucines at positions 815 and 816.

We measured the NF-κB activity of TLR4 (L815AL816A)-EGFP, the mutant in which both leucines were replaced with alanines, under LPS stimulation (Fig. 4*A*). This mutant protein did not respond to LPS stimuli. Microscopic observation revealed that TLR4 (L815AL816A)-EGFP was not expressed on the plasma membrane regardless of whether MD-2 was cotransfected (Fig. 4*B*). The phenotype of this doubly substituted mutant appeared to be the same as that of the truncation mutants. These results imply that the leucines in positions 815 and 816 play an important role in TLR4 plasma membrane localization.

Analysis of Single Amino Acid Substitution Mutants—As previously mentioned, the amino acid sequence leucine-leucine at positions 815 and 816 does not completely match the dileucine motif, *i.e.* it lacks a preceding acidic amino acid. Therefore it